Space: Science & Technology
A SCIENCE PARTNER JOURNAL

SPJ

# Manuscript Template

FRONT MATTER

## Lunar soil maturity of Chang'e-5 samples and its variation with depth

**Authors**

Siyuan Zhao[1], Yuqi Qian[2], Jiawei Zhao[1], Antong Gao[1], Wen Zeng[3], Biao Zhu[3], Qi He[1], Jun Huang[1], Jiannan Zhao[1], Jiang Wang[1], Xingyang She[1], Zhenbing She[1], Long Xiao[1,4]*

**Affiliations**

[1]Hubei Key Laboratory of Planetary Geology and Space Exploration, State Key Laboratory of Geological Processes and Mineral Resources, Planetary Science Institute, School of Earth Sciences, China University of Geosciences, Wuhan 430074, China.

[2]NWU-HKU Joint Center of Earth and Planetary Sciences, Department of Earth and Planetary Sciences, The University of Hong Kong, Hong Kong, China.

[3]Badong National Observation and Research Station of Geohazards, China University of Geosciences, Wuhan, 430074, China.

[4]State Key Laboratory of Lunar and Planetary Sciences, Macau University of Science and Technology, Macao, China.

*Address correspondence to: longxiao@cug.edu.cn

**Abstract**

Lunar soil maturity is a critical proxy for the space weathering state, with vertical maturity profiles providing insights into regolith formation and evolution. However, the maturity characteristics of Chang'e-5 drilled soils remain poorly constrained, and no consensus has been reached regarding the maturity of the scooped soils. The lack of subsurface maturity data hinders comparative studies with Apollo drilled samples and the reconstruction of the complete regolith evolution history. Here, we employed electron paramagnetic resonance to quantify nanophase metallic iron (np-$Fe^0$) content across 0–65 cm depths in Chang'e-5

soils. By leveraging the established the linear correlation between $Fe^0$/FeO and Is/FeO, and corroborating it with petrographic agglutinate content, we obtained consistent maturity trends across all three independent parameters. Scooped and drilled soils exhibit Is/FeO values of 23.7 ± 1.7 and 9–15, respectively, indicating that they are less mature than most of Apollo soils. The observed vertical maturity profile suggests in-situ reworking confined primarily to the upper ~3-23 cm. Furthermore, the overall low maturity is consistent with the estimated formation age (~100 million years ago) of the nearby Xu Guangqi crater, indicating that the 0-65 cm regolith column predominantly originates from this relatively recent impact ejecta deposit.

## INTRODUCTION

The Chang'e-5 mission returned the youngest lunar basalt samples to date, providing a unique opportunity to investigate space weathering processes on a geologically young surface. Extensive research has been conducted to determine the formation age and petrogenesis of these basalts (e.g., [1–8]), and numerous novel space weathering features have been identified within Chang'e-5 soil particles (e.g., [9–15]). However, significant controversy persists regarding the maturity of the Chang'e-5 regolith, a key indicator for cumulative space weathering exposure.

Current maturity assessments present a complex and often contradictory picture. Granulometric analyses suggest a fine mean particle size and good sorting, which were initially interpreted as indicative of higher maturity by comparison to certain Apollo soils [16]. Yet, such direct comparisons may be unreliable due to regional variability in maturity-grain size relationships [17, 18]. Spectroscopic measurements further complicate the narrative, yielding estimates ranging from immature to mature based on in-situ and laboratory spectral data compared to the Lunar Soil Characterization Consortium (LSCC) dataset [19–22]. In contrast, magnetic susceptibility measurements indicate an extremely low metallic iron ($Fe^0$) content, implying an immature state for the scooped soil [23]. This low maturity is further supported by iron isotope analyses, which show less fractionation between Chang'e-5 basalts and soils than observed in Apollo samples, suggesting limited vaporization loss consistent with immature regolith [24]. Conversely, studies of solar flare track densities in olivine grains suggest a mature exposure history [10], while microstructural analysis of ilmenite rims reveals a non-monotonic weathering profile with depth [25]. These significant discrepancies underscore the challenges in consistently assessing the maturity of young lunar soils and underscore the need for a unified analytical approach.

During space weathering, lunar regolith undergoes a systematic evolution: the content of np-$Fe^0$, $Fe^0$, and agglutinates increases, grain size typically decreases; and spectral characteristics darken, redden, and exhibit weakened absorption features [26]. A definitive comparative study of lunar soil maturity indices identified Is/FeO as the most reliable and widely applicable metric [18]. Unlike other indices (e.g., agglutinate content, $Fe^0$/FeO, and mean grain size), Is/FeO—which quantifies the FMR signal from fine-grained np-$Fe^0$ normalized to total FeO—shows no saturation effects and is independent of bulk soil composition. The $Fe^0$/FeO ratio represents a composite signal for maturity studies, encapsulating both a potential meteoritic component and a variable background of indigenous metal that is inherently higher in many highland lithologies [27]. This fundamental limitation limits its utility as a universal maturity index. In contrast, Is/FeO specifically quantifies the fine-grained np-$Fe^0$ generated directly from the in-situ reduction of FeO during surface exposure. This direct genetic link to the space weathering process makes Is/FeO a superior and most reliable proxy for relative exposure age. Its strong correlation with independent exposure age records, such as solar wind nitrogen and argon, confirms its robustness for comparing soil maturity across diverse lunar landing sites. However, applying this established index to Chang'e-5 samples is challenging. Original Is/FeO calibrations were primarily established using Apollo samples analyzed in NASA laboratories, and the relative nature of EPR amplitude measurements complicates direct cross-instrument comparisons in the absence of standard reference materials [23].

To address these issues, this study employs EPR to quantitatively measure the np-$Fe^0$ content in Chang'e-5 soils. By utilizing the strong correlation observed between the $Fe^0$/FeO ratio and the traditional Is/FeO index [23, 28], we determine the maturity of Chang'e-5 scooped and drilled soils, enabling direct comparison with Apollo and Luna data. Furthermore, the consistency among our EPR results, the $Fe^0$/FeO data, and independent petrographic agglutinate counts validates the maturity trends observed. By analyzing samples from depths of 0 to 65 cm, we present the first detailed vertical maturity profile for Chang'e-5 regolith. This profile, corroborated by multiple maturity indices, provides critical insights into the subsurface structure and evolutionary history of the lunar soil at the Chang'e-5 landing site, helps to reconcile previous conflicting evidence and constrains the regolith formation mechanisms in this young geological unit.

## MATERIALS AND METHODS

### Materials

The lunar soil samples used in this study were allocated by the China National Space Administration. These include four drill core samples: CE5Z0709 (from ~23 cm depth), CE5Z0609 (~31 cm), CE5Z0403 (~50 cm), and CE5Z0204 (~65 cm). One group of drill core samples was analyzed using a vibrating sample magnetometer (VSM) to measure the FeO and $Fe^0$ content, while two sets were analyzed via EPR to determine the np-$Fe^0$ content. The EPR and VSM raw data for the scooped soil sample CE5C0600 were originally measured by [23] and reanalyzed here.

### Methods

#### *Vibrating Sample Magnetometer*

The FeO and $Fe^0$ content of lunar soil samples were measured using VSM (see Text S1 for detail). VSM analysis was performed on the four drilled samples: CE5Z0709, CE5Z0609, CE5Z0403, and CE5Z0204. During sample preparation, approximately 35 mg of lunar soil was placed at the bottom of a capsule, and the remaining space was filled with cotton. Measurements were conducted using a Lake Shore 8604 Vibrating Sample Magnetometer at the Institute of Geophysics and Geomatics, China University of Geosciences (Wuhan). The room temperature was maintained at 23°C. Magnetic hysteresis loops were acquired over a magnetic field range of -1.9 to 1.9 T, a step size of 0.01 T, and an integration time of 0.2 seconds.

#### *Electron Paramagnetic Resonance Spectrometer*

The Ferromagnetic Resonance (FMR) spectrum of lunar soil is dominated by the signal from np-$Fe^0$ particles in the size range of 4–33 nm (denoted $Fe^0_A$, [29]), which were primarily formed through the reduction of divalent iron during space weathering processes [28]. The FMR experiments were conducted using a Bruker A300–8/2.7 Electron Paramagnetic Resonance spectrometer at the Badong National Observation and Research Station of Geohazards of China University of Geosciences (Wuhan).

For each of the four drill core samples (CE5Z0709, CE5Z0609, CE5Z0403, and CE5Z0204), two independent sub-samples were prepared. Each sub-sample was loaded into quartz tubes (inner diameter: 0.5 mm), and the tube bottom was sealed with clay. Following weighing, FMR measurements were performed immediately. The EPR instrumental parameters were set as follows: microwave frequency, 9.86 GHz; power, 0.169 mW; scanning field range, 0-1 T; resolution, 1024 (~1 mT); integration time, 100 ms; time constant, 163.84 ms; modulation frequency, 100 kHz; modulation amplitude, 1 mT. All measurements were carried out at a constant room temperature of 22°C. After inserting into the resonant cavity and tuning of the microwave bridge, the quality factor (Q) of the samples was approximately 10,000. Each sample tube was measured twice, being rotated by 90° between measurements to account for any orientation-dependent effects. The FMR data reported for each depth represent the average of these two independent measurements. Post-measurement analysis confirmed that the particle sizes in the tubes were all <250 µm. Additionally, multiple $MnSO_4.H_2O$ standard samples were measured to calibrate the $Fe^0_A$ (see Text S2 and Figure S1 for detailed FMR data processing methods). The EPR data for the scooped sample CE5C0600, originally acquired using the same instrument and parameters [23], were reanalyzed in this study.

### *Agglutinate Abundance Analysis*

The abundance of agglutinates in the 90–150 µm soil fraction is a key maturity indicator for lunar regolith. To quantify this parameter, several hundred particles within the 90–150 µm size range were hand-picked from each of the four drill core samples under a binocular microscope. The separated grain mounts were then analyzed using a TESCAN Integrated Mineral Analyzer (TIMA) at the Hubei Key Laboratory of Planetary Geology and Space Exploration, China University of Geosciences (Wuhan) to obtain Backscattered Electron (BSE) images for subsequent identification and counting of agglutinate particles.

## RESULTS

### FeO and Metallic Iron Content

The theoretical FeO content corresponding to the high-field magnetic susceptibility ($\chi_p$) of lunar samples is generally slightly higher than the chemically measured FeO content (see Text S1 and Figure S2 in the supporting information, [27, 30, 31]). This discrepancy may be attributed to the paramagnetic behavior of some very fine-grained np-$Fe^0$ at room temperature [32]. Nevertheless, FeO content shows a linear relationship with $\chi_p$, and the fitting yields the equation: FeO (wt%) = (49.3 ± 2.0) $\chi_p$ + (1.0 ± 0.5). Based on this fitted relationship, the FeO content derived from $\chi_p$ for samples CE5Z0709, CE5Z0609, CE5Z0403, and CE5Z0204 are 22.0 ± 1.0, 23.5 ± 1.0, 22.9 ± 1.0, and 23.0 ± 1.0, respectively (Table 1). These values are consistent with the reported FeO content of the drill core soil (22.22 wt%, [33]).

The calculated $Fe^0$ contents for the scooped sample CE5C0600 and the drill core samples CE5Z0709, CE5Z0609, CE5Z0403, and CE5Z0204 are 0.422 wt%, 0.264 wt%, 0.270 wt%, 0.230 wt%, and 0.304 wt%, respectively (Table 1). The scooped sample exhibits a significantly higher $Fe^0$ content than all drilled samples.

***Table 1.*** *VSM parameters and maturity of Chang'e-5 sample.*

| Sample | CE5C0600 | CE5Z0709 | CE5Z0609 | CE5Z0403 | CE5Z0204 |
|---|---|---|---|---|---|
| Depth (cm) | 0–3 | 23 | 31 | 50 | 65 |
| Mass (mg) | 6.02 | 35.1 | 34.5 | 38.1 | 36.4 |
| $M_s$ ($Am^2/kg$) | 0.92 | 0.576 | 0.588 | 0.501 | 0.662 |
| $\chi_p$ ($Am^2\ kg^{-1}\ T^{-1}$) | - | 0.424 | 0.455 | 0.443 | 0.444 |
| $Fe^0$ (wt%) | 0.422 [23] | 0.264 | 0.27 | 0.23 | 0.304 |
| FeO (wt%) | 22.22 [33] | 22.0±1.0 | 23.5±1.0 | 22.9±1.0 | 23.0±1.0 |
| $Fe^0$/FeO | 0.019 | 0.0120±0.0005 | 0.0115±0.0005 | 0.0100±0.0004 | 0.0132±0.0006 |
| Is/FeO | 22±4 | 13±4 | 12±4 | 10±4 | 14±4 |

*Ms: saturation magnetization; $\chi_p$: high-field magnetic susceptibility; $Fe^0$: metallic iron content; FeO: iron oxide content.

**FMR Results**

To assess reproducibility, two independent sub-samples were analyzed for each depth interval. The results of two duplicate FMR measurements for the same sample showed excellent consistency, with an average absolute error of 0.1–0.3%. The mean value of the two measurements was presented as the FMR curves for the drilled samples. The mass-corrected FMR spectra of Chang'e-5 sample are shown in Figure 1. The first derivative spectra (Figure 1a, 1c) exhibit an asymmetric shape characterized by a broader and lower left side and a narrower and higher right side. The g-factor (intersection of the first derivative spectra with the x-axis) ranges from 2.07 to 2.08, consistent with values reported for Apollo and Luna lunar soils [34–36]. This spectral profile is predominantly attributed to np-$Fe^0$ particles in the size range of 4-33 nm. The scooped sample has a linewidth ($\Delta H$) of 86.0 mT, whereas the drilled samples exhibit similar linewidths across different depths, ranging from 77.2 to 81.1 mT, which are notably narrower than that of the scooped sample. The FMR absorption spectra (Figure 1b, 1d) of scooped sample exhibit significantly higher absorption intensity than those of the drilled sample. Furthermore, the zero-field absorption intensity of the scooped lunar soil is 2 to 3.5 times greater than that of the drilled samples, indicating a substantially higher content of both 4–33 nm np-$Fe^0$ and larger iron particles (> 33 nm) in the surface samples. Among the drilled samples, the variations in amplitude and absorption intensity are relatively minor. Integrating the results from both measurement sets, the overall trend follows CE5Z0709 ≈ CE5Z0609 > CE5Z0403 ≈ CE5Z0204, with the amplitude and absorption intensity generally decreasing with depth.

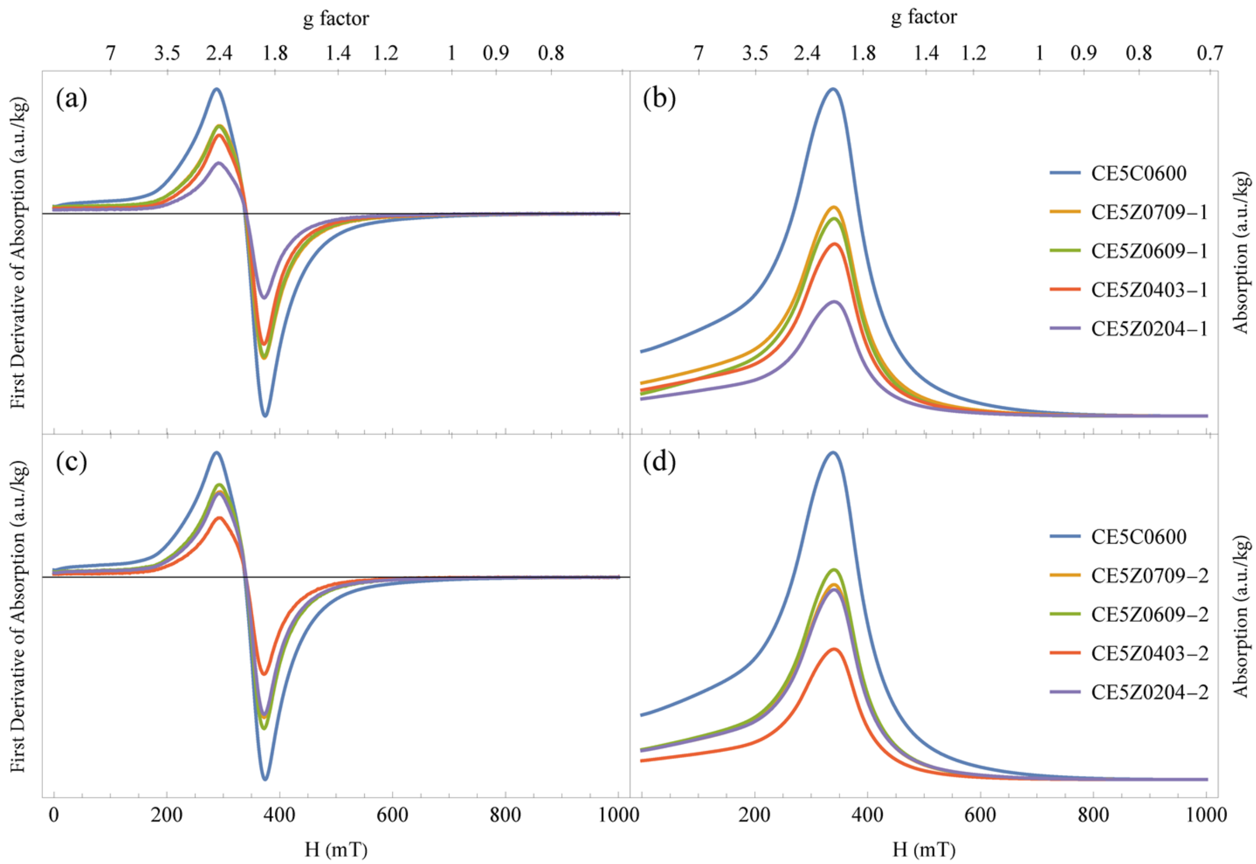


***Fig. 1**. The FMR spectra of Chang'e-5 sample at different depths. The figure includes: (a) First derivative spectra of the first batch of samples, (b) Absorption spectra of the first batch of samples, (c) First derivative spectra of the second batch of samples, and (d) Absorption spectra of the second batch of samples. The original FMR data for the CE5C0600 scooped sample are measured by [23], and have been reprocessed for this study.*

The conversion coefficient (c) between the absorption spectral area and the amount of substance was determined to be (1.40 ± 0.04) × $10^{16}$ by measuring the EPR spectra of four

$MnSO_4 \cdot H_2O$ powder standards (see Figure S3 and Table S1 in the supporting information). The calculated $Fe^0_A$ contents of Chang'e-5 lunar soil are listed in Table 2.

***Table 2.*** *FMR parameters and maturity of Chang'e-5 sample.*

| Sample | CE5C0600 | CE5Z0709-1 | CE5Z0709-2 | CE5Z0609-1 | CE5Z0609-2 | CE5Z0403-1 | CE5Z0403-2 | CE5Z0204-1 | CE5Z0204-2 |
|---|---|---|---|---|---|---|---|---|---|
| Depth (cm) | 0-3 | 23 | 23 | 31 | 31 | 50 | 50 | 65 | 65 |
| Mass (mg) | 16.93 | 2.08 | 2.28 | 2.24 | 2.28 | 2.2 | 1.89 | 1.79 | 4.07 |
| $H_r$ (mT) | 338.2 | 339.5 | 339.9 | 340.1 | 339.8 | 340.9 | 340.1 | 340.3 | 340.1 |
| g factor | 2.08 | 2.07 | 2.07 | 2.07 | 2.07 | 2.07 | 2.07 | 2.07 | 2.07 |
| △H (mT) | 86.0 | 80.2 | 77.2 | 78.2 | 79.2 | 80.2 | 79.1 | 81.1 | 79.1 |
| A/m (a.u./kg) | $9.21\times10^{11}$ | $6.55\times10^{11}$ | $6.36\times10^{11}$ | $6.48\times10^{11}$ | $6.87\times10^{11}$ | $5.88\times10^{11}$ | $4.40\times10^{11}$ | $3.80\times10^{11}$ | $6.22\times10^{11}$ |
| FeO (wt%) | 22.22 | 22.0±1.0 | 22.0±1.0 | 23.5±1.0 | 23.5±1.0 | 22.9±1.0 | 22.9±1.0 | 23.0±1.0 | 23.0±1.0 |
| $Fe^0_A$ (wt%) | 0.161±0.005 | 0.100±0.003 | 0.093±0.003 | 0.096±0.003 | 0.101±0.003 | 0.080±0.002 | 0.063±0.002 | 0.054±0.002 | 0.091±0.003 |
| $Fe^0_A$/FeO | 0.0072±0.0002 | 0.0046±0.0002 | 0.0042±0.0002 | 0.0041±0.0002 | 0.0043±0.0002 | 0.0035±0.0002 | 0.0027±0.0002 | 0.0024±0.0001 | 0.0040±0.0002 |
| Is/FeO | 23.7±1.7 | 15.6±1.6 | 14.7±1.6 | 14.3±1.6 | 14.9±1.6 | 12.5±1.6 | 10.2±1.5 | 9.0±1.5 | 13.9±1.6 |

### Agglutinate Abundance

The abundance of agglutinates, a key maturity indicator, was quantified in the 90–150 μm size fraction of the drill core samples. Representative BSE images illustrating typical agglutinate morphologies are presented in Figure S4. The measured agglutinate proportions are 8.2% (61 out of 739 particles) for CE5Z0709 (23 cm), 10.5% (76/722) for CE5Z0609 (31 cm), 11.1% (68/610) for CE5Z0403 (50 cm), and 8.9% (33/370) for CE5Z0204 (65 cm). These agglutinate counts, all clustering around 10%, are significantly lower than those observed in the vast majority of mature Apollo and Luna soils.

## DISCUSSION

### Maturity of Chang'e-5 samples

*$Fe^0_A$/FeO Index*

The $Fe^0_A$/FeO values of Chang'e-5 samples are listed in Table 2. The $Fe^0_A$/FeO maturity parameter of Apollo and Luna sample is highly correlated with the Is/FeO maturity index [23, 28], and the fitting relationship (Figure 2) is:

$$\text{Is/FeO} = (2990 \pm 75)\, Fe^0_A/\text{FeO} + 2.0 \pm 1.4 \tag{1}$$

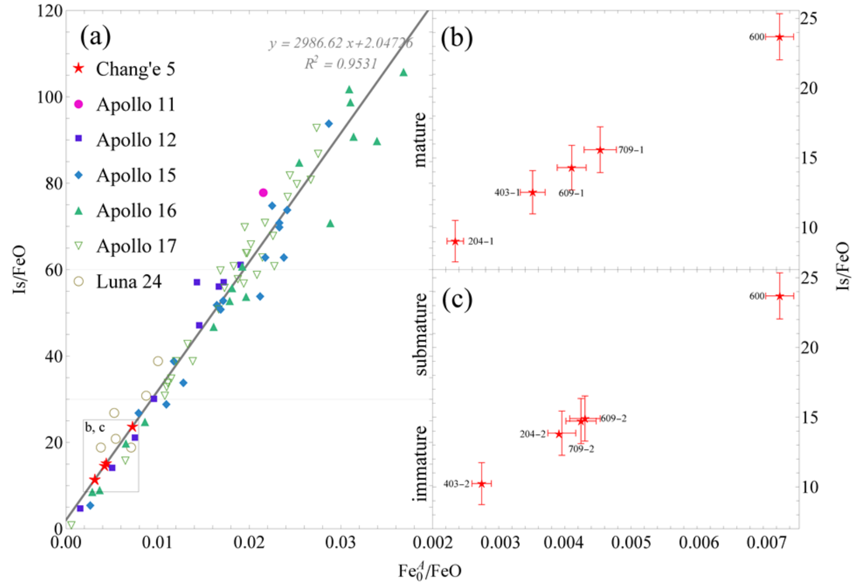


***Fig. 2***. *The comparison of $Fe^0_A$/FeO and Is/FeO between CE 5, Apollo, and Luna samples. The Is/FeO values for Chang'e-5 were estimated from $Fe^0_A$/FeO. The black rectangular area represents the plotting range of b and c. Apollo and Luna data were measured by [28]*

Using this correlation, the Is/FeO value of the scooped sample CE5C0600 is estimated to be 23.7±1.7. For the drilled samples, the two measurement sets yield the following Is/FeO values from shallow to deep: Set 1) 15.6±1.6, 14.3±1.6, 12.5±1.6, and 9.0±1.5; Set 2) 14.7 ±1.6, 14.9±1.6, 10.2±1.5, and 13.9±1.6. The results from the two sets are in good agreement, with differences of 1-5 Is/FeO units for the same sample, likely reflecting sample heterogeneity.

The results demonstrate that the maturity of Chang'e-5 sample at all depths is lower than that of the vast majority of Apollo and Luna samples. The scooped sample is significantly more mature than the drilled samples. The drilled samples themself exhibit uniformly low maturity with little systematic variation. The EPR line width (ΔH) for all Chang'e-5 samples falls within the typical range (~80 mT) and does not show a significant broadening (>>100 mT) associated with thermal alteration. This distinguishes the Chang'e-5 samples from case like the Apollo 68001/2 core sample, where Is/FeO cooccurs with ΔH due to thermal events [37], thereby confirming the genuinely low maturity of the Chang'e-5 samples.

*$Fe^0$/FeO Index*

The Chang'e-5 soils are primarily derived from the local Em4 basalt unit [38–40]. The $Fe^0$ content within pristine basalt fragments is stable across different regolith depths, ranging from 0.08 to 0.10 wt% [23], which is consistent with the range observed in most Apollo mare basalts (0.026–0.167 wt% [41]). In contrast, the Apollo 16 landing site is situated in the feldspathic highlands, where some anorthosites and gabbroic rocks inherently contain significantly higher native metal contents (Figure 3), reaching up to ~1 wt% [27], far exceeding values typical of mare basalts. To establish a robust $Fe^0$/FeO and Is/FeO correlation specifically for mare regolith, we performed a linear regression using data from Apollo mare samples while explicitly excluding the compositionally anomalous Apollo 16 highland soils. The resulting best-fit relationship is:

$$Is/FeO = (1343.47 \pm 88.63)Fe^0/FeO - 3.40 \pm 3.81$$

Applying this mare-specific calibration, the equivalent Is/FeO maturity values for the Chang'e-5 samples CE5C0600, CE5Z0709, CE5Z0609, CE5Z0403, and CE5Z0204 are calculated to be 22 ± 4, 13 ± 4, 12 ± 4, 10 ± 4, and 14 ± 4, respectively. These results uniformly classify all Chang'e-5 soils as immature. Furthermore, they confirm that the maturity of the drilled soils (23–65 cm) is uniformly low and show little variation, whereas the scooped soil (0–3 cm) is slightly more mature.

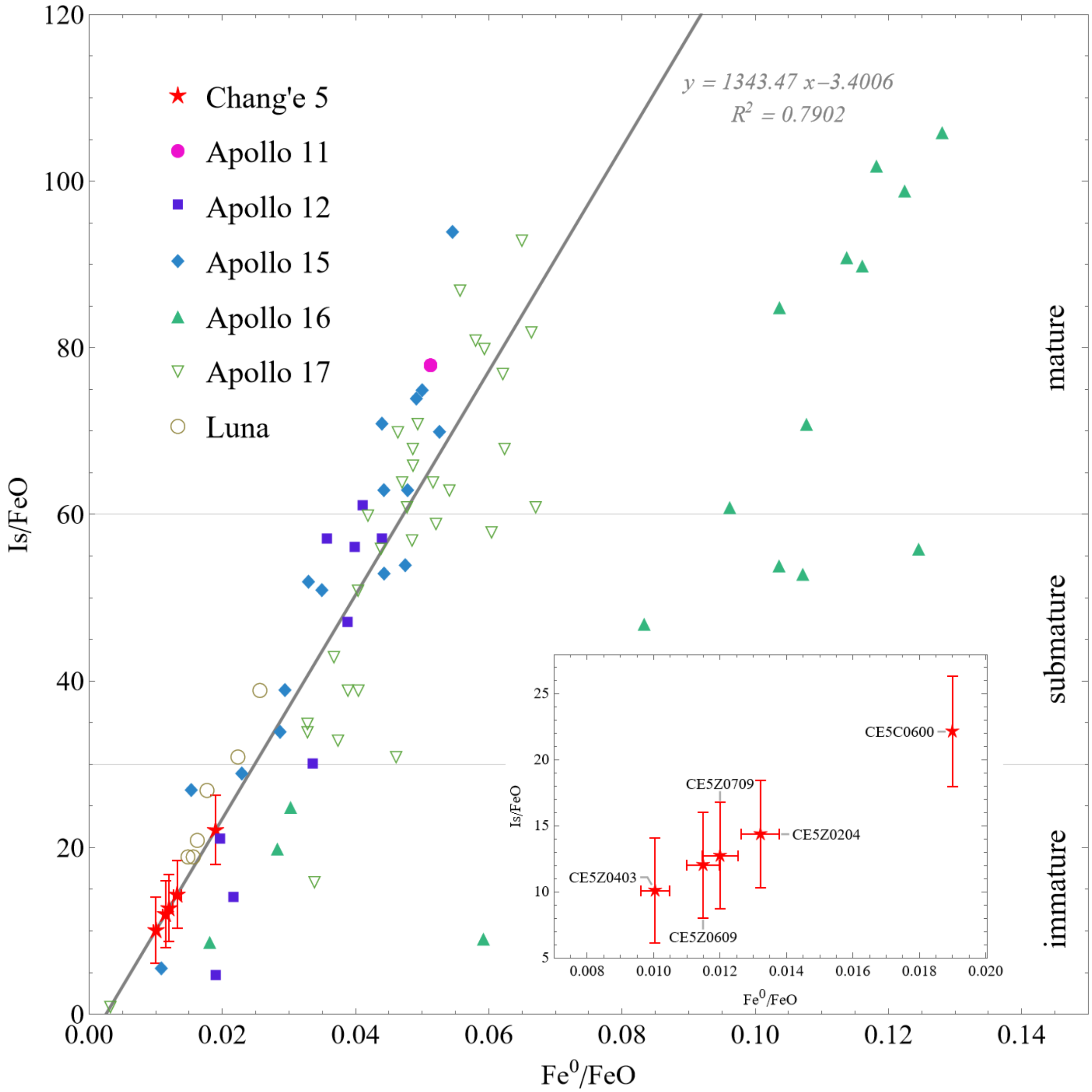


***Fig. 3***. *The comparison of $Fe^0/FeO$ and Is/FeO between Chang'e-5, Apollo, and Luna samples. The Is/FeO values for Chang'e-5 were estimated from $Fe^0/FeO$. Apollo and Luna data were measured by [28]*

*Agglutinate Index*

We derived a maturity index for the Chang'e-5 soils based on the established correlation between petrographic agglutinate abundance and Is/FeO in lunar soil studies [18]. Although agglutinate content is known to saturate at high maturity levels, the notably immature Chang'e-5 samples lie well within the early, quasi-linear phase of the agglutinate–Is/FeO relationship, where saturation effects are negligible. Fitting the agglutinate content (90–150 μm fraction) against the Is/FeO values of the <250 μm fraction yields the linear regression of Is/FeO = 1.36 × agglutinate abundance (Figure 4). This relationship reliably reflects the immature nature of the Chang'e-5 regolith and allows for a meaningful estimation of its surface exposure history. The equivalent Is/FeO values for CE5Z0709, CE5Z0609, CE5Z0403, and CE5Z0204 are calculated to be 11 ± 3, 14 ± 3, 15 ± 3, and 12 ± 3, respectively, consistently classifying all drilled Chang'e-5 soils as immature.

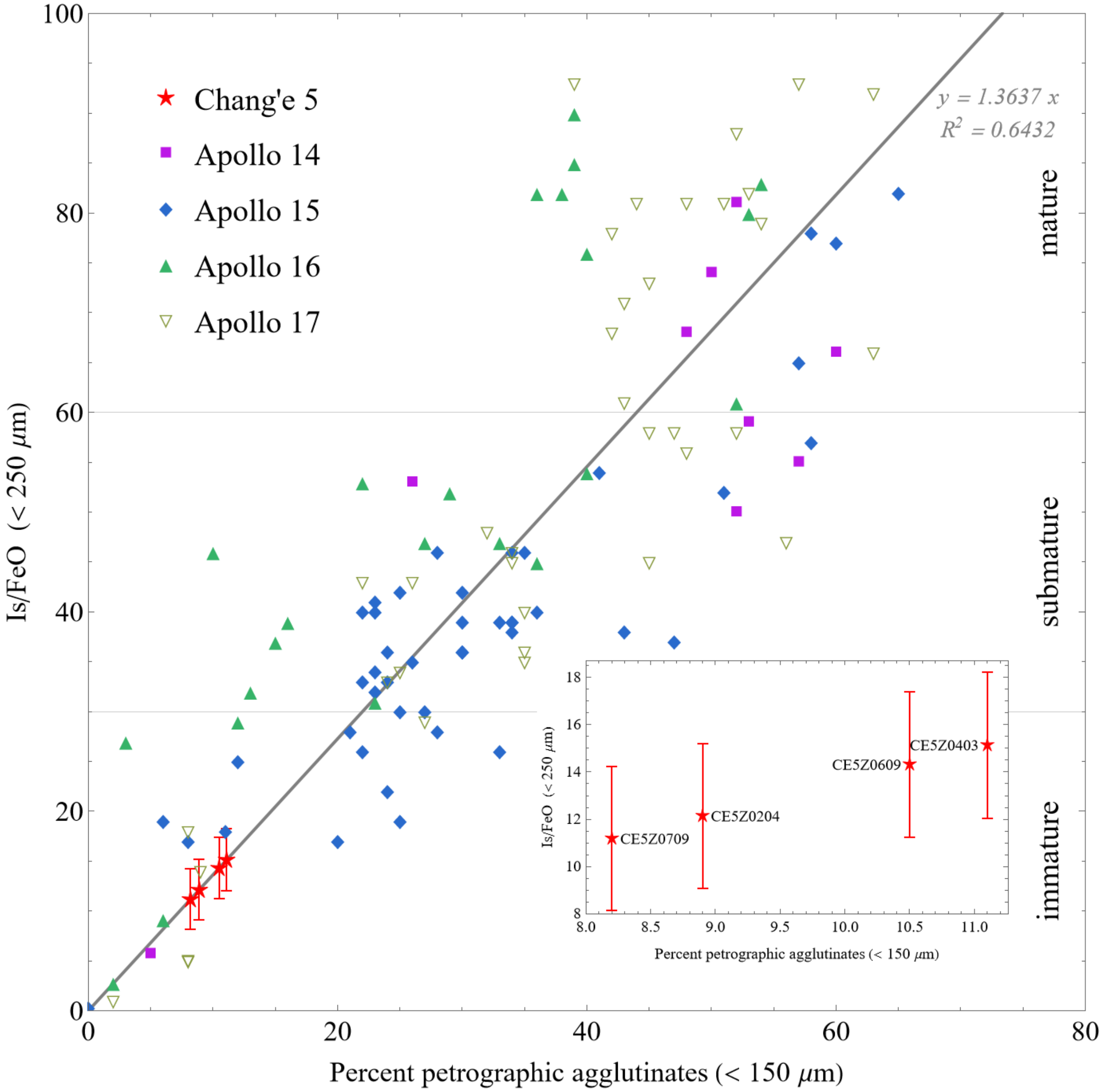


***Fig. 4***. *The comparison of percent petrographic agglutinates and Is/FeO between CE 5, Apollo, and Luna samples. The Is/FeO values for Chang'e-5 were estimated from agglutinate. Apollo and Luna data were measured by* [18]

***Comparison of Different Maturity Indices***

The maturity of the Chang'e-5 samples was assessed using three independent indices: the $Fe^0_A$/FeO ratio (from EPR), the $Fe^0$/FeO ratio (from saturation magnetization), and the petrographic agglutinate abundance. A comparative analysis reveals a highly consistent maturity pattern with depth. For the scooped sample (CE5C0600), the $Fe^0_A$/FeO and $Fe^0$/FeO indices yield Is/FeO value of 23.7 ± 1.7 and 22 ± 4, respectively. For the drilled samples (CE5Z0709, CE5Z0609, CE5Z0403, CE5Z0204), the $Fe^0_A$/FeO and $Fe^0$/FeO, and agglutinate indices of range between 9-16, 10-14, and 11-15, respectively.

The convergence of these three independent maturity indicators provides evidence for two key findings: (1) the scooped soil (0–3 cm) exhibits a significantly higher maturity than the underlying drilled soils; (2) the drilled soils from 23 cm to 65 cm display uniformly low and similar maturity levels, with no discernible correlation with depth. The consistent classification of the 23–65 cm drill core as "immature" by all three methods underscores that this section of the regolith has experienced minimal space weathering and has been effectively shielded from surface reworking processes, preserving its initial state since deposition.

The maturity of the scooped soil reported in this study align with assessments based on iron isotopic compositions [23, 24], but exhibits significant discrepancies in optical maturity metrics (see Table S2). For instance, Qian et al. [23] derived an equivalent Is/FeO value of ~14 using a different Is/FeO vs. $Fe^0$/FeO ($Fe^0/FeO = 5.88\times10^{-4}$ Is/FeO + 0.0105) correlation, which is slightly lower than the maturity values obtained in our study (22±4) but still consistent in general and confirm the overall immaturity of the Chang'e-5 scooped lunar soils. Recalibrating their data using our mare-specific relationship (Is/FeO = 1343.47 $Fe^0$/FeO – 3.40) yields an equivalent Is/FeO value of ~22, closely matching our results. The minor iron isotopes fractionation between Chang'e-5 basalt and scooped soil further supports the low maturity of the scooped soil [24].

Regarding the vertical maturity profile, Guo et al. [25] report that lower weathering intensity at 26–45 cm depths compared to the surface layer (0–3 cm) is based on only two ilmenite samples from that horizon, only one of which showed significant weathering features. The limited sampling introduces substantial statistical uncertainty, as such sporadic, highly weathered grains could be inherited from pre-existing mature material (Layer 1 in Figure 6) rather than representing in-situ space weathering processes at that depth.

The discrepancies in optical maturity estimates across different studies likely arise from two main factors:

(1) Methodological inconsistencies: The lack standardized protocols for optical maturity assessments, combined with limited spectral-maturity reference data in the Lunar Soil Characterization Consortium (LSCC) dataset, amplifies variablity between different methods.

(2) Grain size effects: Maturity indices are know to be inversely correlated with grain size [18, 42]. For example, Lu et al. [21] demonstrated that fine fractions yield higher maturity values than coarse fractions, underscoring the critical influence of particle size selection in spectral measurements.

**Source of agglutinates in Chang'e-5 the sample**

The linewidth (ΔH) of lunar soils shows a positive correlation with FeO content of the agglutinate glass. Since agglutinates typically have compositions consistent with surrounding soils, Apollo samples define a well-established linear ΔH-FeO trend (see Figure S6, [18]). An empirical fit to Apollo and Luna soils yields: FeO (wt%) = (0.488 ± 0.021) ΔH – (21.5 ± 1.4). Deviations from this trend occur when the FeO content of the agglutinate glass differs from the bulk soil composition. For example, a section of the Apollo 17 deep drill core (26–60 cm) has elevated FeO, yet its ΔH values align with those underlying, low-FeO layers. This anomaly has been interpreted as evidence of contamination by low-FeO agglutinate glass [43]. The bulk FeO content of Chang'e-5 soils form different depth is relatively uniform. The scooped sample lies close to the established ΔH-FeO trend, while as the drilled samples exhibit significantly lower ΔH values. This divergence suggests distinct provenances for the agglutinates: those in the scooped soils are primarily derived from the in-situ weathering of local basaltic material, while agglutinates in the drilled soils may be partially or wholly sourced from FeO-depleted exotic component (e.g., materials from craters such as Harpalus, Copernicus, Aristarchus crater materials [44]) incorporated via vertical mixing.

**The provenance of Chang'e-5 regolith**

Compared to the scooped soil sample (Is/FeO ~24), the Chang'e-5 lunar soil at depths of 23–65 cm shows lower maturity (Is/FeO: 9-16), fluctuating within a narrow range. Apollo 15 deep core, 60009/10, 74001/2, and Apollo 17 deep drill core (see Figure S7, [45–49]) have high-maturity zones at the top of the cores caused by in-situ reworking. In-situ reworking (gardening) involves the continual reworking of the uppermost regolith by micrometeoroid bombardment, which mechanically mix the soil and introduce mature materials—such as agglutinates, np-$Fe^0$ and $Fe^0$—to some depth. The top layer (<3 mm) Chang'e-5 maturity is higher than the deeper section (23-65 cm), and the profile is similar to the in-situ reworked Apollo cores, indicating that in-situ reworking also has occurred in the Chang'e-5 core. The observed similarity in maturity profiles, particularly the presence of a near-surface zone with elevated Is/FeO values, supports the interpretation that the Chang'e-5 site has experienced a comparable regolith evolution process. The stable low maturity of the lunar soil at depths of 23 cm and below indicates that this section of lunar soil has undergone minimal disturbance since its formation and the soil at depths of 0–65 cm may have been formed by a single impact event or multiple events within a short period of time. Due to the lack of specific constraints on the lunar soil between 3 cm and 23 cm, it is speculated that the in-situ reworking depth ($D_r$) of the Chang'e-5 soil profile is estimated to be between 3 and 23 cm.

Morris et al. [48] proposed a function relationship (see Figure 5 and Table S3 in the supporting information) between the $D_r$ (cm) and exposure age (Ma):

$$D_r = 2.2t^{0.45} \quad (2)$$

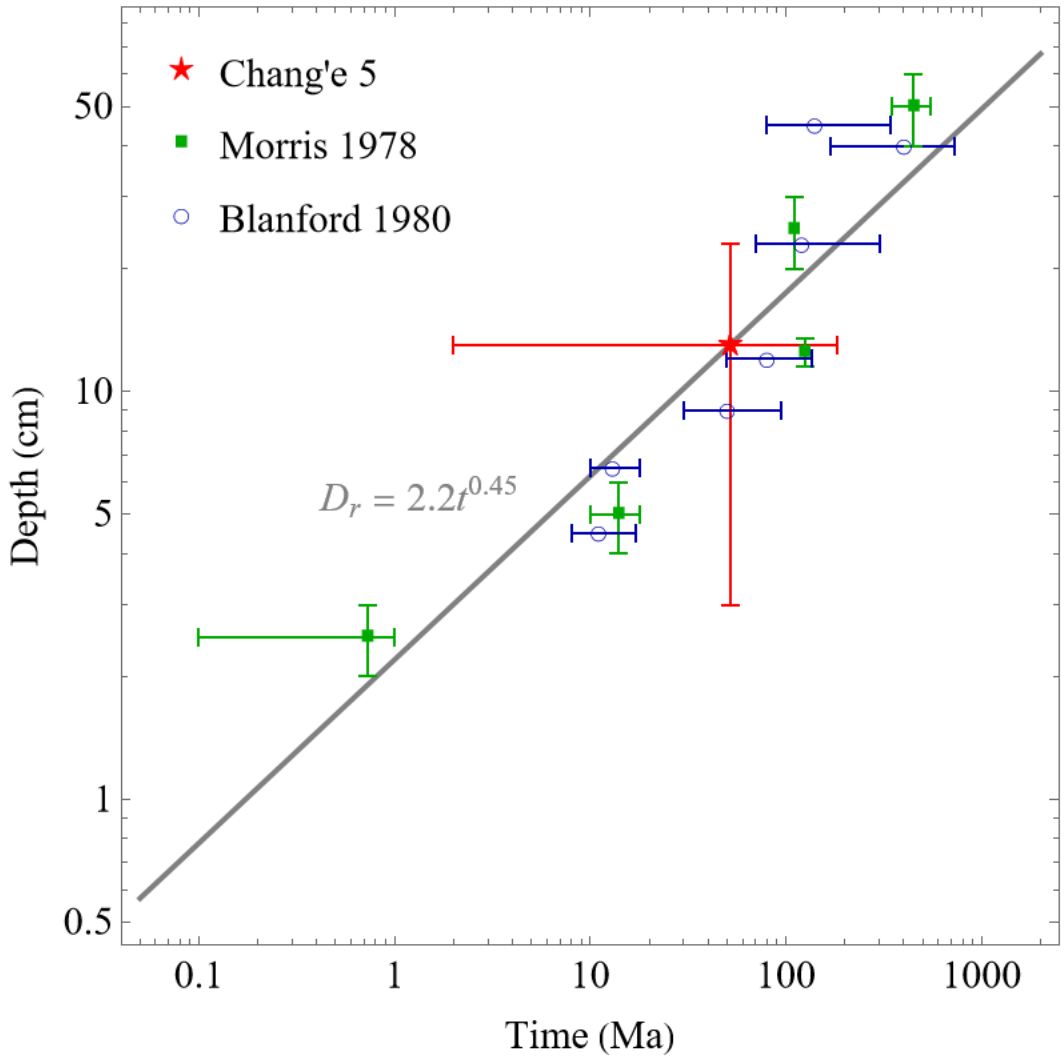


***Fig. 5***. *The $D_r$ of the lunar core and the exposure age of the lunar regolith. Apollo data are sourced from [47] and [50].*

The provenance of the shallower subsurface materials at the Chang'e-5 landing site has been previously proposed to be dominated by ejecta from the nearby Xu Guangqi crater, based on morphological and crater distribution studies [39, 44, 51]. This crater exhibits a degradation age of 60–218 Ma and an absolute model age of ~46 Ma [39, 44]. The in-situ reworking depth ($D_r$) in our core corresponds to an exposure age of $52^{+132}_{-50}$ Ma for the Chang'e-5 shallow regolith. This exposure age shows notable consistency with the formation age of the Xu Guangqi crater, providing independent support for the proposed genetic link between the crater and the surficial regolith at the landing site. These converging lines of evidence support the interpretation that the 0–65 cm regolith profile at Chang'e-5 predominantly originated from the Xu Guangqi impact event. A potential contribution from the adjacent, smaller C2 crater (diameter ~100 m) has also been suggested to account for part of the regolith thickness [39, 44]. Although the small size of C2 precludes precise crater size-frequency distribution dating, both degradation age analysis and morphological age estimates suggest that C2 and Xu Guangqi craters formed within comparable time intervals [44]. Therefore, while the Xu Guangqi event is considered the primary source, the shallower regolith may represent a cumulative deposit potentially incorporating ejecta from both the Xu Guangqi and C2 craters-a distinction our data cannot definitively resolve. The overall low maturity of the drill core samples is consistent with a regolith column dominated by ejecta from these relatively recent impact events.

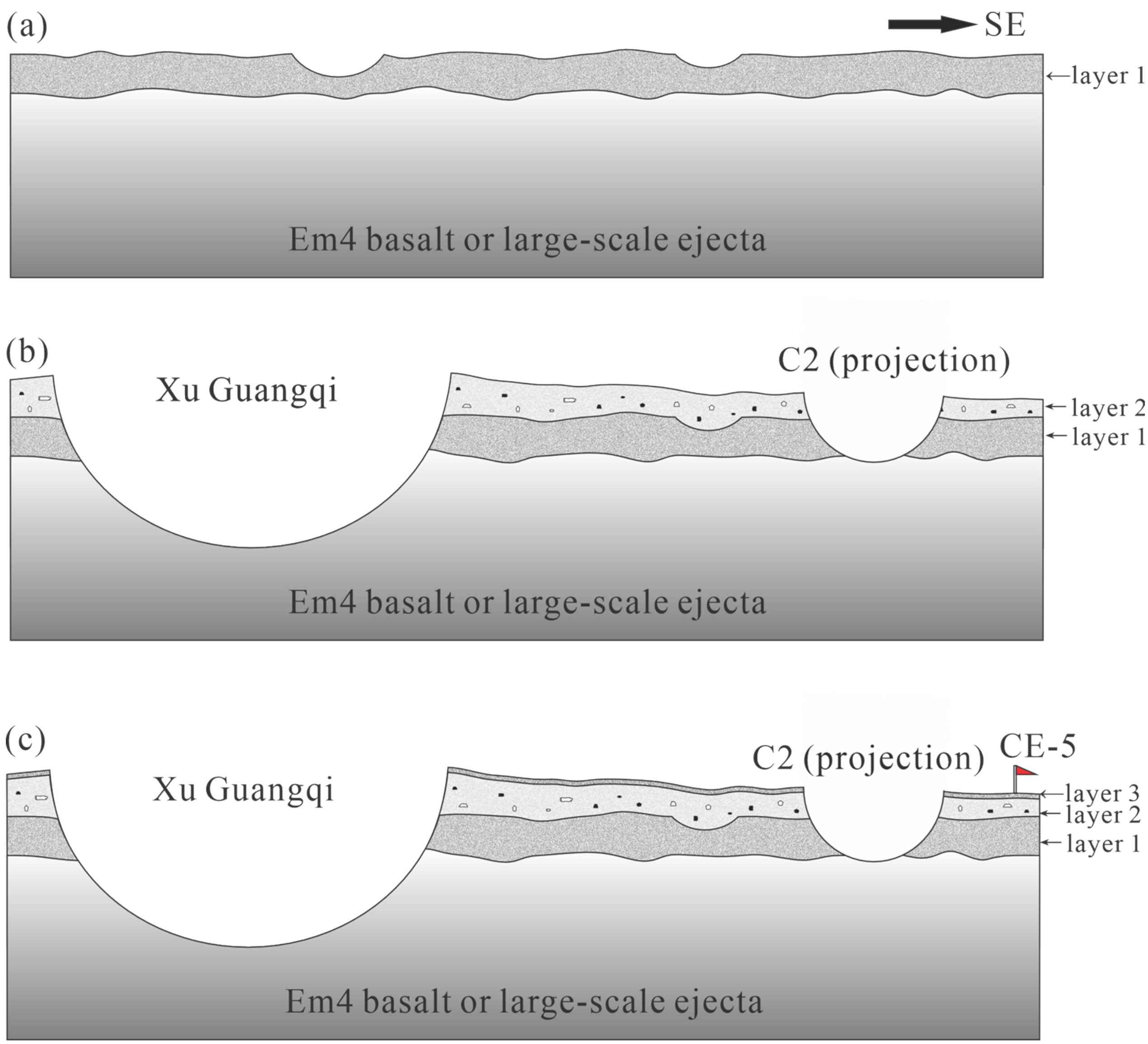


***Fig. 6**. Schematic of regolith formation processes at the Chang'e-5 landing site (not in scale). (a) A pre-existing regolith layer (several meters thick, layer 1) developed at the landing site prior to the formation of Xu Guangqi. (b) Xu Guangqi crater excavated fresh*

*materials under the layer 1, forming a new regolith layer (layer 2) containing: remobilized materials from layer 1 and impact-derived boulders, coarse-grained ejecta components. The thickness of layer 2 is at least 65 cm at the Chang'e-5 landing site. (c) Post space weathering progressively altered the superficial regolith (3-23 cm thick, layer 3) of layer 2.*

Therefore, based on the observed maturity profile and chronological constraints, the regolith formation sequence at the Chang'e-5 landing site as follows (Figure 6):

(1) Pre-Xu Guangqi Basement: Prior to the Xu Guangqi crater formation, a mature regolith layer (Layer 1, several meters thick) had developed atop the Em4 basalt or an older ejecta substrate. This paleoregolith incorporated FeO-depleted materials potentially sourced from distal impact events, representing over >1.8 Ga of cumulative space weathering.

(2) Xu Guangqi Ejecta Emplacement: The Xu Guangqi impact event (<200 Ma) excavated fresh subsurface materials from beneath layer 1, depositing a new ejecta blanket (Layer 2). This layer is characterized by a mixture of dominate coarse-grained, pristine ejecta and remobilized mature components from the underlying Layer 1. At the sampling site, Layer 2 exceeds 65 cm in thickness.

(3) Post-impact Surface Weathering: Following the impact, space weathering progressively matured the superficial regolith, forming a distinct zone of higher maturity within upper ~3-23 cm of Layer 2.

## CONCLUSION

This study provides a quantitative characterization of the space weathering history of Chang'e-5 lunar regolith (0-65 cm depth) through integrated analyses of np-$Fe^0$ content via electron paramagnetic resonance spectroscopy and FeO abundance (via electron vibrating sample magnetometry). We established a robust linear correlation between $Fe^0_A$ /FeO and Is/FeO ratios, enabling a reliable determination of regolith maturity. The scooped sample exhibits higher maturity (Is/FeO = 24) compared to drilled samples (Is/FeO = 9-16), confirming the overall immaturity of Chang'e-5 regolith within the investigated profile. Two distinct layers are identified: (1) an in-situ reworking layer (upper ~3- 23 cm) shows relative maturation signatures from recent surface weathering; and (2) an undisturbed layer (23-65 cm), which preserves pre-impact compositional characteristics. The exposure age of the reworking layer ($52^{+132}_{-50}$Ma) aligns with the Xu Guangqi crater's formation age

(46-218 Ma), which is consistent with its role as the primary regolith source of the upper 65 cm regolith at the Chang'e-5 landing site.


## ACKNOWLEDGMENTS

**General**: We thank China National Space Administration (CNSA) for implementing the Chang’e-5 mission and providing access to the Chang’e-5 samples. The authors express thanks to the anonymousreviewers for their insightful and constructive comments and suggestions. The authors are grateful to Professor Huiru Xu for her expert guidance on the operation of the Vibrating Sample Magnetometer.

**Author contributions:** S. Z.: Conceptualization, Methodology, Investigation, Formal Analysis, Visualization, Writing – Original Draft; Y. Q.: Writing – Review & Editing, Funding Acquisition; J. Z.: Investigation; A. G.: Investigation; W. Z.: Resources; B. Z.: Investigation; Q. H.: Resources; J. H.: Investigation; J. Z.: Investigation; J. W.: Investigation; X. S.: Investigation; Z. S.: Resources; L. X.: Conceptualization, Writing – Review & Editing, Resources, Supervision, Funding Acquisition.

**Funding:** This work was supported by National Key R&D Program of China [grant numbers 2023YFB3711300] and the Science and Technology Development Fund of Macau [grant numbers 0052/2024/RIA1, 0021/2024/RIA1 and 0158/2024/AF]. Yuqi Qian was funded by the Seed Fund for Basic Research for New Staff [grant numbers 2401102770] and HK RGC grants [grant numbers 17307025 and 17308023].

**Competing interests:** The authors declare that there is no conflict of interest regarding the publication of this article.


## DATA AVAILABILITY

Electron Paramagnetic Resonance (EPR), Vibrating Sample Magnetometer (VSM) and Backscattered Electron (BSE) data of Chang’e-5 lunar soil samples (CE5Z0204, CE5Z0403, CE5Z0609 and CE5Z0709) are available from figshare (https://doi.org/10.6084/m9.figshare.29552219).

## SUPPLEMENTARY MATERIALS

Text S1 to S2

**Text S1.**

The magnetic hysteresis loop is the B-M curve acquired when magnetic particles are subjected to a cyclic external magnetic field. Lunar soil contains both ferromagnetic materials (such as $Fe^0$, which exhibits a hysteresis loop, Figure S5) and paramagnetic materials (such as $Fe^{2+}$-bearing minerals or glass, whose B-M curve is a reversible straight line with a constant slope). Therefore, the B-M curve of lunar soil (i.e., the uncorrected hysteresis loop) shows a closed region (the hysteresis loop) where the slope gradually decreases with increasing field strength at low fields. When the field strength increases to a certain level, the curve closes into a straight line with a constant slope, which is defined as the high-field magnetic susceptibility $\chi_p$. In lunar soils, $\chi_p$ is positively correlated with the FeO content (wt%) of lunar sample, with a theoretical value of FeO = 50.91 $\chi_p$. This formula closely matches the FeO content measured by chemical methods when $\chi_p$ is below 0.2, but the predicted FeO content becomes significantly overestimated when $\chi_p$ exceeds 0.2 (Figure S2). This error may be due to superparamagnetic iron, as the "hysteresis loop" of superparamagnetic iron shows a decrease in magnetic susceptibility at high fields but does not reach zero, leading to an overestimation of FeO content. The higher the FeO content in the lunar regolith, the more likely it is to produce superparamagnetic iron, thus high-FeO samples are more prone to deviate from the theoretical value [27]. Here, we fit the high-field magnetic susceptibility $\chi_p$ of Apollo lunar samples with the FeO content measured by chemical methods, and the fitting function is as follows:

$$\mathrm{FeO} = (49.3 \pm 2.0)\,\chi^p + 1.0 \pm 0.5$$

Removing the influence of paramagnetic susceptibility yields a corrected hysteresis loop (Figure S5), which better reflects the intrinsic magnetic properties of the ferromagnetic components. When the hysteresis loop closes at high fields, the magnetization no longer increases with the applied field, and the corresponding magnetization value is defined as the saturation magnetization ($M_s$). The saturation magnetization of $Fe^0$ is 218 $A\cdot m^2/kg$. Assuming that $Fe^0$ is the only magnetic phase in lunar soil, the $Fe^0$ content can be estimated as $Fe^0$ (wt%) = $M_s/2.18$.

**Text S2.**

The FMR first derivative spectrum obtained from the EPR spectrometer may show a shift, manifested as the tail of the curve being above or below the x-axis (Figure S1a), and thus need to be corrected. The correction is done by subtracting the average value of the last 50 points from the uncorrected spectrum. After correction, the difference between the maximum and minimum values of the intensity on the y-axis gives the amplitude A (dimensionless), the difference on the x-axis between these two points gives the linewidth ΔH (mT), and the intersection of the spectrum and the x-axis between these two points represents the applied magnetic field at resonance $H_r$ (mT) (Figure S1b). The relationship between the g-factor (also known as the g-value, dimensionless) and $H_r$ is given by the following formula:

$$h\nu = g\beta H_r$$

where h is the Planck constant ($6.626\times10^{-34}$ J s), ν is the microwave frequency (Hz), and β is the Bohr magneton ($9.274\times10^{-24}$ J/T). The absorption spectrum is obtained by integrating the first derivative spectrum, with the integration starting from the last point and accumulating backwards:

$$y^1_{1024} = 0,\ y^1_{1024-i} = y^1_{1025-i} - y^1_{1024-i}$$

The area enclosed by the absorption spectrum in the main absorption range (180–560 mT, Figure S1c) is positively correlated with np- $Fe^0$ in the 4–33 nm range ($Fe^0_A$ [28]). By calibrating the absorption area with $MnSO_4\cdot H_2O$, the absolute contents of $Fe^0_A$ can be obtained. Housley et al. provided a detailed method for correction [29]. In summary, the relationship between the enclosed area of np- $Fe^0$, $A_{Fe}$ and the amount of np-$Fe^0$, $n_{Fe}$ is:

$$A_{Fe} = c\,\mu_{eff}\,\beta\,N_A\,n_{Fe}$$

where $\mu_{eff}$ represents the effective magnetic moment of $Fe^0$, with a value of 2.18 [29]; β is the Bohr magneton ($9.274 \times 10^{-24}$ J/T); $N_A$ is Avogadro's constant ($6.022 \times 10^{23}$ $mol^{-1}$); c is a constant ($J^{-1}$ T), related to the instrument and test parameters, and can be obtained through measurement with $MnSO_4\cdot H_2O$. The relationship between the area enclosed by the absorption spectrum of $MnSO_4\cdot H_2O$, $A_{Mn}$, and the amount of $MnSO_4\cdot H_2O$, $n_{Mn}$ is given by:

$$A_{Mn} = \frac{c\,n_{Mn}\,g\,\beta\,N_A\,S\,(S + 1)\,h\nu}{3k\,(T - \theta)}$$

where g is the g-factor of $MnSO_4\cdot H_2O$, which is measured to be 2.00 in this experiment; S = 5/2; k is the Boltzmann constant ($1.380 \times 10^{-23}$ J/K); T is the absolute temperature of the test environment (295.15 K); and θ is the Curie constant (-26 K, [52]) Figures S1 to S6

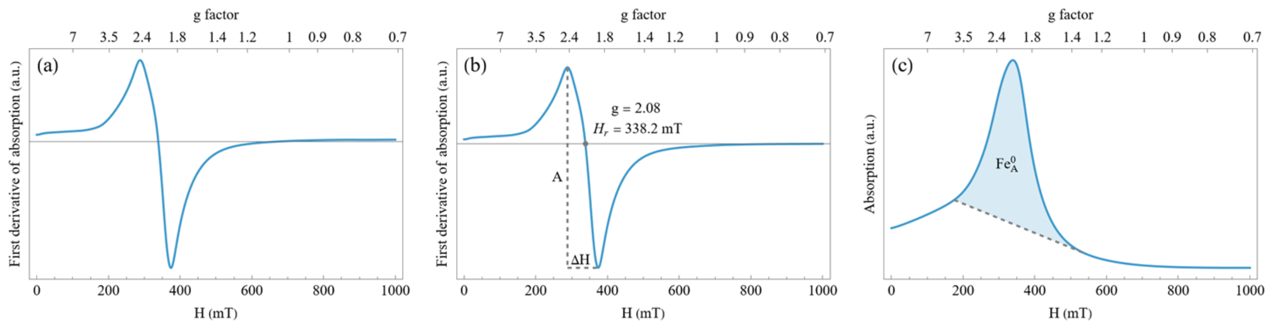


**Figure S1.** The processing of FMR data. (a) The uncorrected first derivative spectrum (the end of this curve is above or below the x-axis); (b) The corrected first derivative spectrum (the end of the curve is close to the x-axis); (c) The area of the main absorption interval of the absorption spectrum represents the content of (4–33 nm) in the lunar regolith.

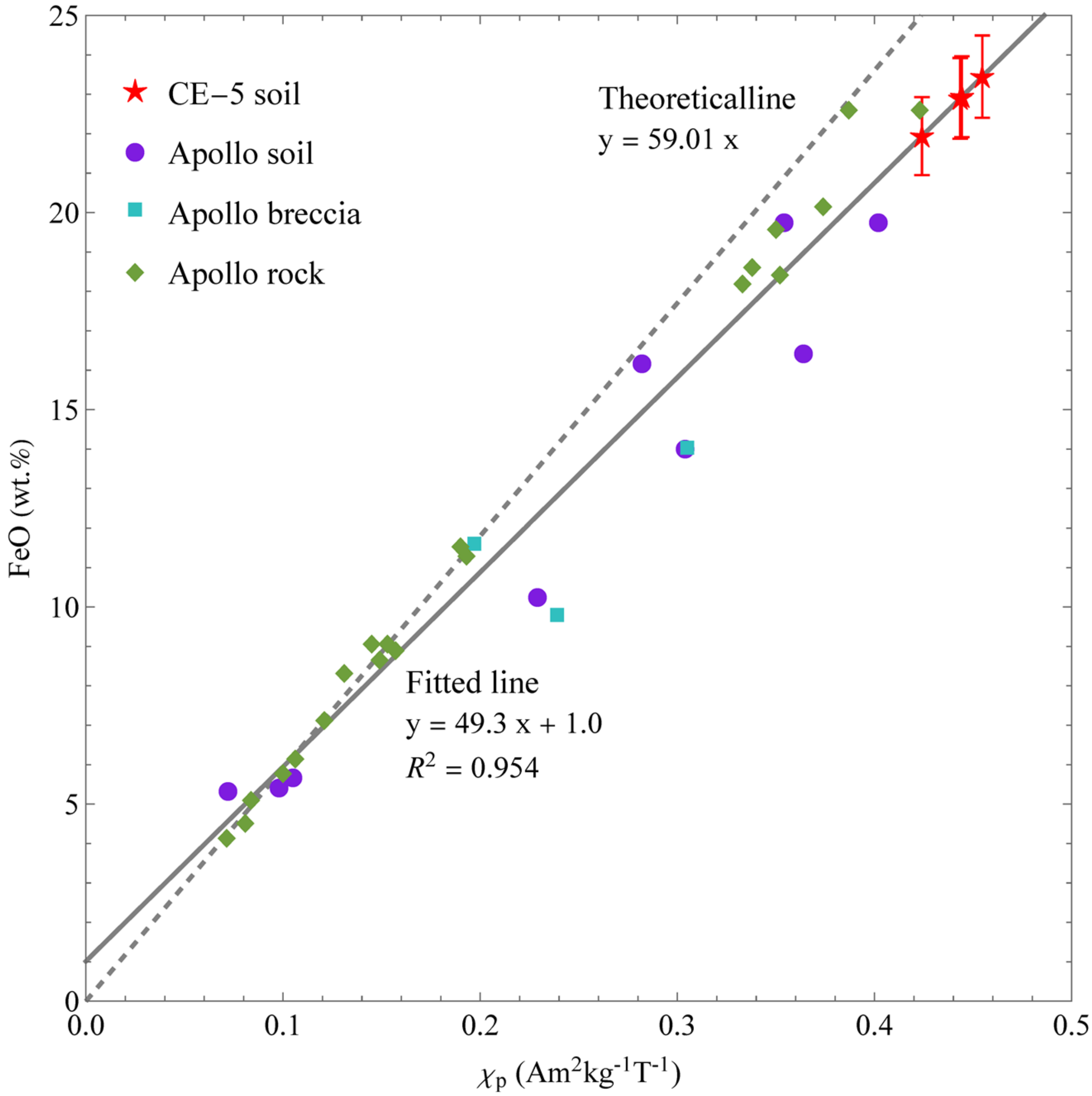


**Figure S2.** Relationship between high-field magnetic susceptibility ($\chi_p$) and FeO content measured by chemical methods for Apollo lunar samples, along with high-field magnetic susceptibility of Chang'e-5 drill core samples. The dashed line represents the theoretical relationship, and the solid line represents the fitted curve. Apollo data sources: [27, 30, 31]

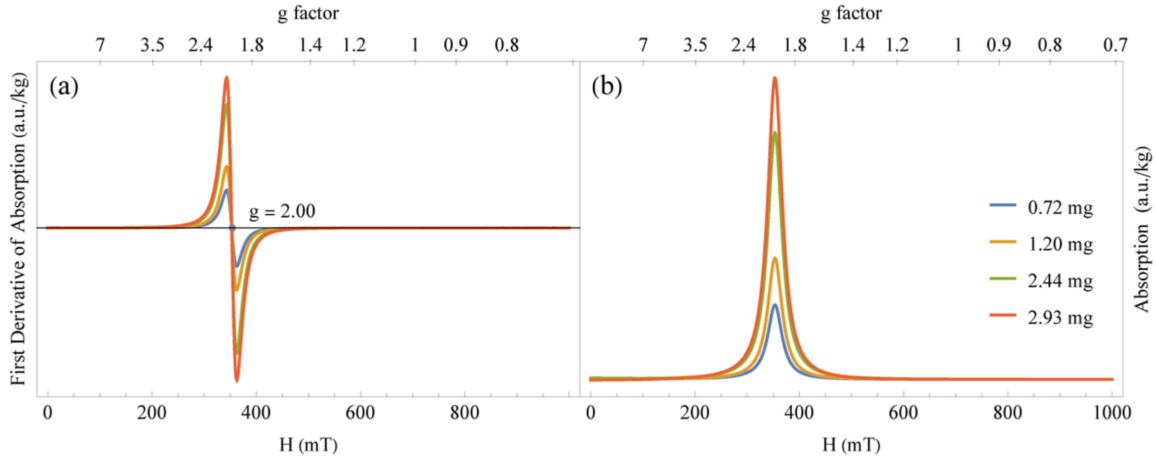


**Figure S3.** EPR (a) first derivative spectra and (b) absorption spectra of MnSO4·H2O standard samples with different masses.

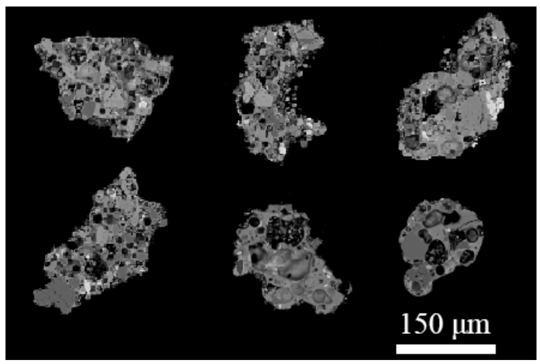


**Figure S4.** Representative BSE images of agglutinates in Chang’e-5 lunar soil samples.

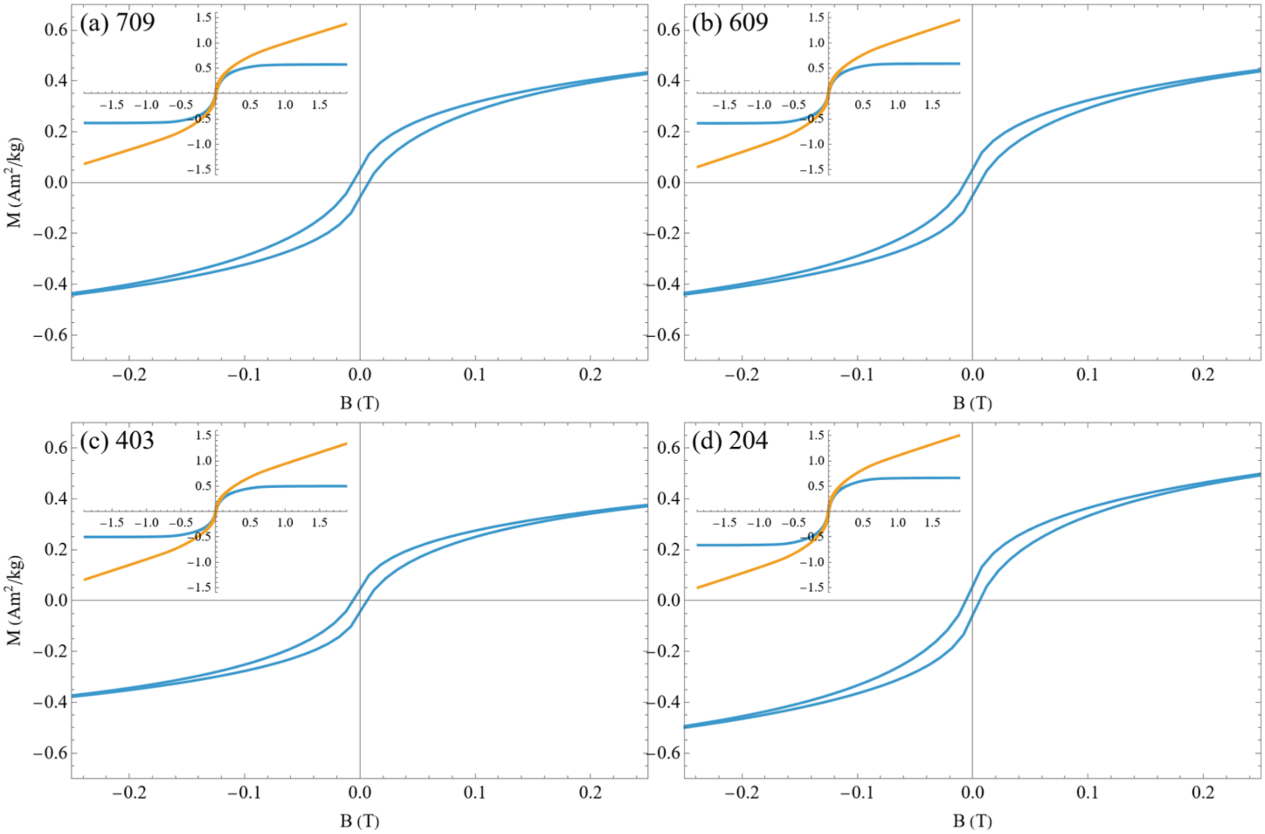


**Figure S5.** The raw hysteresis loop (orange) and paramagnetically corrected hysteresis loop (blue) of (a) CE5Z0709, (b) CE5Z0609, (c) CE5Z0403, and (d) CE5Z0204.

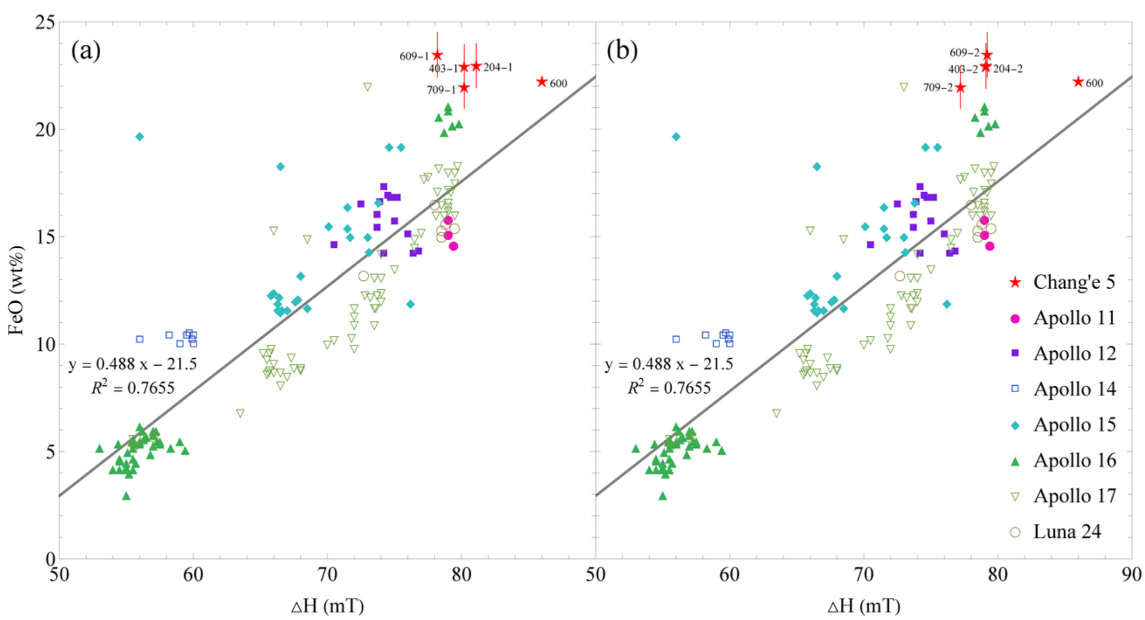

**Figure S6.** The relationship between the line width ΔH of different lunar soils and the FeO content. Apollo and Luna soil data sourced from [53], and the CE5C0600 data sourced from [23].

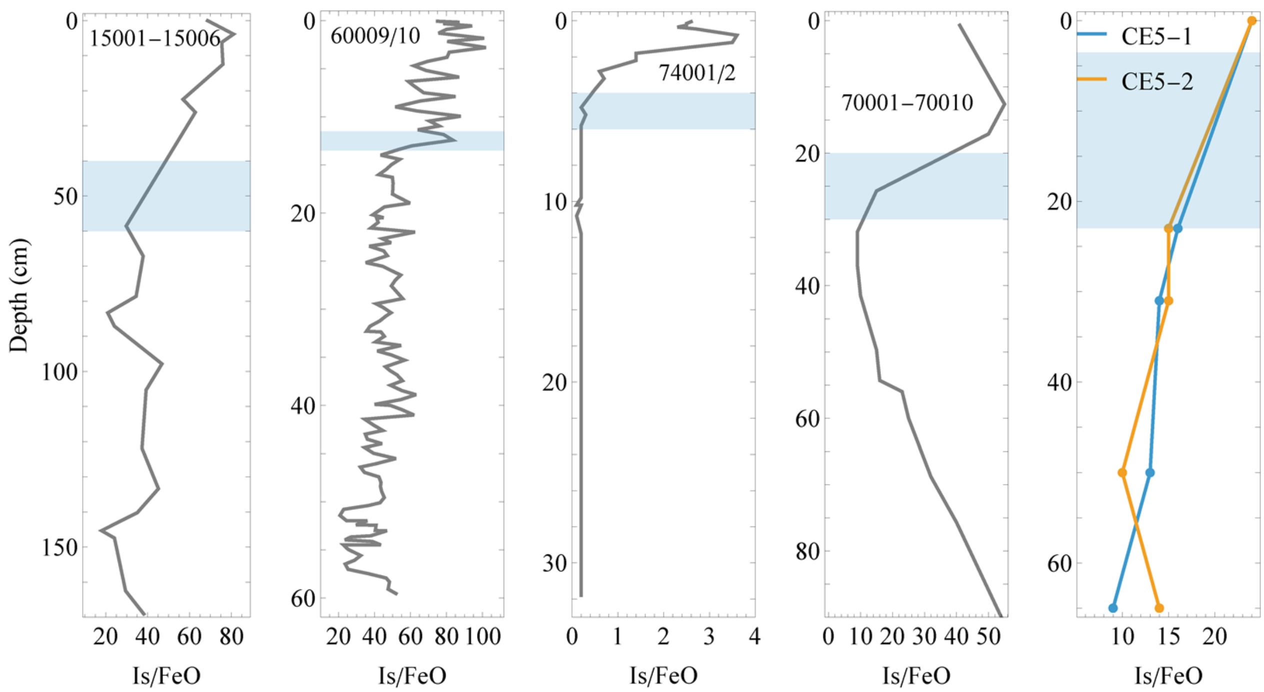


**Figure S7**. The maturity profile comparison between Apollo and Chang'e-5. The range of in-situ reworking depth marks with lightblue rectangular areas. The maturity data for the Apollo samples are sourced from [45–49]

Tables S1 to S3

**Table S1.** The relationship between the EPR absorption area and the amount of substance for MnSO4·H2O standard samples

| Mass (mg) | Amount of substance (mol) | Absorption area (a.u./kg) | c |
|---|---|---|---|
| 0.72 | 0.122 | $2.971\times10^{9}$ | $1.454\times10^{16}$ |
| 1.20 | 0.202 | $4.667\times10^{9}$ | $1.370\times10^{16}$ |
| 2.44 | 0.412 | $9.636\times10^{9}$ | $1.391\times10^{16}$ |
| 2.93 | 0.495 | $1.1349\times10^{10}$ | $1.364\times10^{16}$ |

**Table S2.** The maturity of Chang'e-5 soil

| Depth | Maturity Index | Equivalent Is/FeO | Maturity | References |
|---|---|---|---|---|
| 0-3 cm | Grain size | (>60) | Mature | [54] |
| 0-3 cm | Optical maturity (< 25μm) | 66.4 | Mature | [19] |

| | | | | |
|---|---|---|---|---|
| 0-3 cm | Optical maturity (< 1 mm) | 16 | Immature | [19] |
| 0-3 cm | Optical maturity (in-situ) | 25-38 | Immature-submature | [19] |
| 0-3 cm | Optical maturity (in-situ) | (30-60) | Submature | [20] |
| 0-3 cm | Optical maturity (in-situ, < 45µm, 45-355µm, bulk) | (30-60) | Submature | [21] |
| 0-3 cm | Optical maturity (< 45µm) | 62 | Mature | [22] |
| 10 cm | Optical maturity (< 45µm) | 46 | Submature | [22] |
| 0-3 cm | $Fe^0$(> 2-4 nm)/FeO | 14 | Immature | [23] |
| 0-3 cm | Olivine rim | (>60) | Mature | [10] |
| 0-3 cm | Fe isotope | (0-30) | Immature | [24] |
| 0-3 cm | $Fe_A^0$/FeO | 24±2 | Immature | This work |
| 23 cm | $Fe_A^0$/FeO | 16±2/15±2 | Immature | This work |
| 31 cm | $Fe_A^0$/FeO | 14±2/15±2 | Immature | This work |
| 45 cm | $Fe_A^0$/FeO | 13±2/10±2 | Immature | This work |
| 65 cm | $Fe_A^0$/FeO | 9±2/14±2 | Immature | This work |
| 0-3 cm | $Fe^0$(> 2-4 nm)/FeO | 22±4 | Immature | This work |
| 23 cm | $Fe^0$(> 2-4 nm)/FeO | 13±4 | Immature | This work |
| 31 cm | $Fe^0$(> 2-4 nm)/FeO | 12±4 | Immature | This work |
| 45 cm | $Fe^0$(> 2-4 nm)/FeO | 10±4 | Immature | This work |
| 65 cm | $Fe^0$(> 2-4 nm)/FeO | 14±4 | Immature | This work |
| 23 cm | Agglutinate Index | 11±3 | Immature | This work |
| 31 cm | Agglutinate Index | 14±3 | Immature | This work |
| 45 cm | Agglutinate Index | 15±3 | Immature | This work |
| 65 cm | Agglutinate Index | 12±3 | Immature | This work |

**Table S3.** The relationship between in-situ reworking depth and exposure time. Apollo data are sourced from [48] and [50].

| Core | In-situ reworking depth (cm) | Time (Ma) |
|---|---|---|
| Chang'e-5 | 13 ± 10 | - |
| Apollo 15 deep dill core (15001–15006) | 50 ± 10 | 450 ± 100 |
| | 40 | $400^{+330}_{-230}$ |

| | | |
|---|---|---|
| | 45 | $140^{+200}_{-60}$ |
| Apollo 16 60009/10 | 12.5 ± 1.0 | 125 |
| | 12 | $80^{+55}_{-30}$ |
| Apollo 16 deep dill core (60007-60001) | 9 | $50^{+45}_{-20}$ |
| Apollo 17 deep dill core (70001–70009) | 25 ± 5 | 110 |
| | 23 | $120^{+180}_{-50}$ |
| Apollo 17 74001/2 | 5 ± 1 | 14±4 |
| | 4.5 | $11^{+6}_{-5}$ |
| | 6.5 | $13^{+5}_{-3}$ |
| Apollo $^{26}$Al profiles | $0.73^{+0.27}_{-0.63}$ | 2.5 ± 0.5 |

## REFERENCES


[1] Che X, Nemchin A, Liu D, Long T, Wang C, Norman MD, et al. Age and composition of young basalts on the Moon, measured from samples returned by Chang'e-5. Science. 2021;374:887–90. doi:10.1126/science.abl7957.

[2] Hu S, He H, Ji J, Lin Y, Hui H, Anand M, et al. A dry lunar mantle reservoir for young mare basalts of Chang'E-5. Nature 2021. doi:10.1038/s41586-021-04107-9.

[3] Li Q, Zhou Q, Liu Y, Xiao Z, Lin Y, Li J, et al. Two billion-year-old volcanism on the Moon from Chang'E-5 basalts. Nature 2021. doi:10.1038/s41586-021-04100-2.

[4] Tian H, Wang H, Chen Y, Yang W, Zhou Q, Zhang C, et al. Non-KREEP origin for Chang'e-5 basalts in the Procellarum KREEP Terrane. Nature. 2021;600:59–63. doi:10.1038/s41586-021-04119-5.

[5] He Q, Li Y, Baziotis I, Qian Y, Xiao L, Wang Z, et al. Detailed petrogenesis of the unsampled Oceanus Procellarum: The case of the Chang'e-5 mare basalts. Icarus. 2022;383:115082. doi:10.1016/j.icarus.2022.115082.

[6] Chen Y, Hu S, Li J, Li Q, Li X, Li Y, et al. Chang'e-5 lunar samples shed new light on the Moon. The Innovation Geoscience. 2023;1:100014. doi:10.59717/j.xinn-geo.2023.100014.

[7] Luo B, Wang Z, Song J, Qian Y, He Q, Li Y, et al. The magmatic architecture and evolution of the Chang'e-5 lunar basalts. Nature Geoscience. 2023;16:301–8. doi:10.1038/s41561-023-01146-x.

[8] Wu F-Y, Li Q-L, Chen Y, Hu S, Yue Z-Y, Zhou Q, et al. Lunar evolution in light of the Chang'e-5 returned samples. Annual Review of Earth and Planetary Sciences. 2024;52:159–94. doi:10.1146/annurev-earth-040722-100453.

[9] Guo J-G, Ying T, Gao H, Chen X, Song Y, Lin T, et al. Surface microstructures of lunar soil returned by Chang'e-5 mission reveal an intermediate stage in space weathering process. Science Bulletin. 2022;67:1696–701. doi:10.1016/j.scib.2022.06.019.

[10] Guo Z, Li C, Li Y, Wen Y, Tai K, Li X, et al. Nanophase iron particles derived from fayalitic olivine decomposition in Chang'e‐5 lunar soil: implications for thermal effects during impacts. Geophysical Research Letters. 2022;49:e2021GL097323. doi:10.1029/2021GL097323.

[11] Guo Z, Li C, Li Y, Wen Y, Wu Y, Jia B, et al. Sub-microscopic magnetite and metallic iron particles formed by eutectic reaction in Chang'E-5 lunar soil. Nature Communications. 2022;13:7177. doi:10.1038/s41467-022-35009-7.

[12] Li C, Guo Z, Li Y, Tai K, Wei K, Li X, et al. Impact-driven disproportionation origin of nanophase iron particles in Chang’e-5 lunar soil sample. Nature Astronomy. 2022;6:1156–62. doi:10.1038/s41550-022-01763-3.

[13] Xian H, Zhu J, Yang Y, Li S, Lin X, Xi J, et al. Ubiquitous and progressively increasing ferric iron content on the lunar surfaces revealed by the Chang’e-5 sample. Nature Astronomy. 2023;7:280–6. doi:10.1038/s41550-022-01855-0.

[14] He Q, Hu W, Xiao L, Zhang X, Wang Z, Qian Y, et al. Tadpole‐shaped nanoparticles in impact melt and implication of high temperature chemical garden in lunar soil. Journal of Geophysical Research: Planets. 2024;129:e2024JE008584. doi:10.1029/2024JE008584.

[15] Shi Q, He Y, Zhu J-M, Wang Y, Wu H, Wang P, et al. Elemental differentiation and isotopic fractionation during space weathering of Chang’E-5 lunar soil. Geochimica et Cosmochimica Acta. 2024;378:127–43. doi:10.1016/j.gca.2024.06.011.

[16] Zhou C, Jia Y, Liu J, Li H, Fan Y, Zhang Z, et al. Scientific objectives and payloads of the lunar sample return mission—Chang’E-5. Advances in Space Research. 2022;69:823–36. doi:10.1016/j.asr.2021.09.001.

[17] Mendell WW, McKay DS. A lunar soil evolution model. The moon. 1975;13:285–92. doi:10.1007/BF00567520.

[18] Morris RV. Surface exposure indices of lunar soils-A comparative FMR study. In: 7th Lunar Science Conference; 1976. p. 315–335.

[19] Lu X, Chen J, Ling Z, Liu C, Fu X, Le Qiao, et al. Mature lunar soils from Fe-rich and young mare basalts in the Chang'e-5 regolith samples. Nature Astronomy. 2022;7:142–51. doi:10.1038/s41550-022-01838-1.

[20] Wu X, Liu Y, Yang Y, Guo D, Du J, Li S, et al. Mineralogy and regolith maturity at the Chang'E-5 landing site inferred from the Lunar Mineralogical Spectrometer. Earth and Planetary Science Letters. 2022;594:117747. doi:10.1016/j.epsl.2022.117747.

[21] Chang R, Lin H, Yang W, Ruan R, Liu X, Tian H, Xu J. Comparison of laboratory and in-situ reflectance spectra of Chang'e-5 lunar soil. Astronomy & Astrophysics. 2023;674:A68. doi:10.1051/0004-6361/202245751.

[22] Wu Y, Chai Y, Lu Y, Chen X, Wang W, Jin Q. Visible and near-infrared spectral results of Chang'e-5 surficial and subsurface soils. Astronomy & Astrophysics. 2024;682:A112. doi:10.1051/0004-6361/202347577.

[23] Qian Y, Xiao L, Zhao J, Head JW, He Q, Xu H, et al. First magnetic and spectroscopic constraints on attenuated space weathering at the Chang'e-5 landing site. Icarus. 2024;410:115892. doi:10.1016/j.icarus.2023.115892.

[24] Li Y, Wang Z, Qian Y, Zhang W, Feng Y, Liu H, et al. Iron isotopes of Chang'e-5 soil and mineral components: Implications for post-eruption processes on lunar surface. Icarus. 2025;426:116362. doi:10.1016/j.icarus.2024.116362.

[25] Guo Z, Zhang M, Jia B, Li Y, Fa W, Pang Y, et al. Space-weathered rims on lunar ilmenite as an indicator for relative exposure ages of regolith. Communications Earth & Environment. 2024;5:1–9. doi:10.1038/s43247-024-01590-6.

[26] Pieters CM, Noble SK. Space weathering on airless bodies. Journal of Geophysical Research: Planets. 2016;121:1865–84. doi:10.1002/2016JE005128.

[27] Pearce GW, Gose WA, Strangway DW. Magnetic studies on Apollo 15 and 16 lunar samples. In: 4th Lunar Science Conference; 17 Mar 1973; The Woodlands, Houston, Texas. New York, NY: Pergamon Press; 1973.

[28] Morris RV. Origins and size distribution of metallic iron particles in the lunar regolith. In: 11th Lunar and Planetary Science Conference; 17-21 Mar 1980; The Woodlands, Houston, Texas. New York, NY: Pergamon Press; 1980.

[29] Housley RM, Cirlin EH, Crowe H, Goldberg IB. Ferromagnetic resonance studies of lunar core stratigraphy. In: 7th Lunar Science Conference; 1976.

[30] Apollo 17 Preliminary Examination Team. Apollo 17 lunar samples: chemical and petrographic description. Science. 1973;182:659–72. doi:10.1126/science.182.4113.659.

[31] Pearce GW, Strangway DW, Gose WA. Magnetic properties of Apollo samples and implications for regolith formation. In: 5th Lunar Science Conference; The Woodlands, Houston, Texas. New York, NY: Pergamon Press; 1974.

[32] Nagata T, Fisher RM, Schwerer FC, Fuller MD, Dunn JR. Magnetic properties and natural remanent magnetization of Apollo 15 and 16 lunar materials. In: 4th Lunar Science Conference; 17 Mar 1973; The Woodlands, Houston, Texas. New York, NY: Pergamon Press; 1973.

[33] Zong K, Wang Z, Li J, He Q, Li Y, Becker H, et al. Bulk compositions of the Chang'E-5 lunar soil: Insights into chemical homogeneity, exotic addition, and origin of landing site basalts. Geochimica et Cosmochimica Acta. 2022;335:284–96. doi:10.1016/j.gca.2022.06.037.

[34] Tsay F-D, Chan SI, Manatt SL. Ferromagnetic resonance of lunar samples. Geochimica et Cosmochimica Acta. 1971;35:865–75. doi:10.1016/0016-7037(71)90001-9.

[35] Weeks RA. Magnetic phases in lunar material and their electron magnetic resonance spectra: Apollo 14. In: 3th Lunar Science Conference; 1972.

[36] Housley RM, Cirlin EH, Goldberg IB, Crowe H. Ferromagnetic resonance as a method of studying the micrometeorite bombardment history of the lunar surface. In: 7th Lunar Science Conference; 1975.

[37] Korotev RL, Morris RV, Jolliff BL, Schwarz C. Lithological variation with depth and decoupling of maturity parameters in Apollo 16 regolith core 68001/2. Geochimica et Cosmochimica Acta. 1997;61:2989–3002. doi:10.1016/S0016-7037(97)00140-3.

[38] Qian Y, Xiao L, Wang Q, Head JW, Yang R, Kang Y, et al. China's Chang'e-5 landing site: Geology, stratigraphy, and provenance of materials. Earth and Planetary Science Letters. 2021;561:116855. doi:10.1016/j.epsl.2021.116855.

[39] Jia B, Fa W, Zhang M, Di K, Xie M, Tai Y, Li Y. On the provenance of the Chang'E-5 lunar samples. Earth and Planetary Science Letters. 2022;596:117791. doi:10.1016/j.epsl.2022.117791.

[40] Zhao S, Xiao L, Qian Y, Zhao J, She Z, He Q, et al. Variations in lunar regolith properties with depth as revealed by Chang'e-5 samples. Icarus. 2023;406:115766. doi:10.1016/j.icarus.2023.115766.

[41] Strauss BE, Tikoo SM, Gross J, Setera JB, Turrin B. Constraining the decline of the lunar dynamo field at ≈3.1 Ga through paleomagnetic analyses of Apollo 12 mare basalts. Journal of Geophysical Research: Planets 2021. doi:10.1029/2020JE006715.

[42] McKay DS, Dungan MA, Morris RV, Fruland RM. Grain size, petrographic, and FMR studies of the double core 60009/10-A study of soil evolution. In: 8th Lunar Science Conference; 1977.

[43] Morris RV, Lauer HV, Jr, Gose WA. Characterization and depositional and evolutionary history of the Apollo 17 deep drill core. In: 10th Lunar and Planetary Science Conference; The Woodlands, Houston, Texas. New York, NY: Pergamon Press; 1979.

[44] Qian Y, Xiao L, Head JW, Wöhler C, Bugiolacchi R, Wilhelm T, et al. Copernican ‐ aged (<200 ma) impact ejecta at the Chang'e ‐ 5 landing site: statistical evidence from crater morphology, morphometry, and degradation models. Geophysical Research Letters 2021. doi:10.1029/2021GL095341.

[45] Heiken GH, Morris RV, McKay DS, Fruland RM. Petrographic and ferromagnetic resonance studies of the Apollo 15 deep drill core. In: 7th Lunar Science Conference; 1976.

[46] Morris RV, Gose WA. Ferromagnetic resonance and magnetic studies of cores 60009/60010 and 60003-Compositional and surface-exposure stratigraphy. In: 7th Lunar Science Conference; 1976.

[47] Morris RV, Gose WA, Lauer HV, JR. Depositional and surface exposure history of the Shorty Crater core 74001/2-FMR and magnetic studies. In: 9th Lunar and Planetary Science Conference; 17 Mar 1978; The Woodlands, Houston, Texas. New York, NY: Pergamon Press; 1978.

[48] Morris RV. In-situ reworking gardening of the lunar surface-Evidence from the Apollo cores. In: 9th Lunar and Planetary Science Conference; 17 Mar 1978; The Woodlands, Houston, Texas. New York, NY: Pergamon Press; 1978.

[49] Morris RV, Gose WA, Lauer HV, JR. Maturity and FeO profiles for the Apollo 17 deep drill core. In: 9th Lunar and Planetary Science Conference; 17 Mar 1978; The Woodlands, Houston, Texas. New York, NY: Pergamon Press; 1978.

[50] Blanford GE. Cosmic ray production curves below reworking zones. In: 11th Lunar and Planetary Science Conference; 17-21 Mar 1980; The Woodlands, Houston, Texas. New York, NY: Pergamon Press; 1980.

[51] Liu D, Hu T, Kang Z, Hong Y, Liu X. Relationship of the spatial distribution between craters and rocks in the Chang'e−5 landing area based on landing camera images. Planetary and Space Science. 2023;237:105766. doi:10.1016/j.pss.2023.105766.

[52] Allain Y, Krebs JP, Gunzbourg J de. Magnetic study of the manganous sulfates MnSO4 and MnSO4·H2O. Journal of Applied Physics. 1968;39:1124–5. doi:10.1063/1.1656193.

[53] Morris RV. The surface exposure maturity of lunar soils: Some concepts and Is/FeO compilation. In: 9th Lunar and Planetary Science Conference; 17 Mar 1978; The Woodlands, Houston, Texas. New York, NY: Pergamon Press; 1978.

[54] Li C, Hu H, Yang M-F, Pei Z-Y, Zhou Q, Ren X, et al. Characteristics of the lunar samples returned by Chang’e-5 mission. National Science Review 2022. doi:10.1093/nsr/nwab188.

Space: Science & Technology
A SCIENCE PARTNER JOURNAL

# Lunar soil maturity of Chang'e-5 samples and its variation with depth

Siyuan Zhao, Yuqi Qian, Jiawei Zhao, Antong Gao, Wen Zeng, Biao Zhu, Qi He, Jun Huang, Jiannan Zhao, Jiang Wang, Xingyang She, Zhenbing She, and Long Xiao

**Citation:** Zhao S, Qian Y, Zhao J, Gao A, Zeng W, Zhu B, He Q, Huang J, Zhao J, Wang J, et al. Lunar soil maturity of Chang'e-5 samples and its variation with depth. *Space Sci Technol*.**Just Accepted Manuscript** DOI: 10.34133/space.0618



*Space: Science & Technology* (ISSN 2692-7659) is published by the American Association for the Advancement of Science. 1200 New York Avenue NW, Washington, DC 20005.